View metadata, citation and similar papers at core.ac.uk

brought to you by CORE

provided by Elsevier - Publisher Connector

Current Biology, Vol. 13, 1159–1168, July 15, 2003, ©2003 Elsevier Science Ltd. All rights reserved. DOI 10.1016/S0960-9822(03)00451-2

Live Imaging of Endogenous RNA Reveals a Diffusion and Entrapment Mechanism for *nanos* mRNA Localization in *Drosophila*

Kevin M. Forrest and Elizabeth R. Gavis*
Department of Molecular Biology
Princeton University
Princeton, New Jersey 08544

Summary

Background: Localization of *nanos* mRNA to the posterior pole of the *Drosophila* embryo directs local synthesis of Nanos protein that is essential for patterning of the anterior-posterior body axis and germ cell function. While *nanos* RNA is synthesized by the ovarian nurse cells and appears at the posterior pole of the ooctye late in oogenesis, the mechanism by which this RNA is translocated to and anchored at the oocyte posterior is unknown.

Results: By labeling endogenous *nanos* RNA with GFP, we have been able to follow the dynamic pathway of *nanos* localization in living oocytes. We demonstrate that *nanos* localization initiates immediately upon nurse cell dumping, whereby diffusion, enhanced by microtubule-dependent cytoplasmic movements, translocates *nanos* RNA from the nurse cells to the ooctye posterior. At the posterior, *nanos* is trapped by association, in particles, with the posteriorly localized germ plasm. Actin-dependent anchoring of *nanos* RNA complexed to the germ plasm at the posterior maintains localization in the face of rapid cytoplasmic movements.

Conclusions: These results reveal a diffusion-based, late-acting posterior localization mechanism for long-range transport of *nanos* mRNA. This mechanism differs from directed transport-based localization mechanisms in its reliance on bulk movement of RNA.

Introduction

The generation of asymmetry during development and the polarization of differentiated cells require asymmetric distributions of cytoplasmic proteins. Intracellular mRNA localization provides a powerful mechanism to target or restrict synthesis of such proteins to particular subcellular domains. In *Drosophila*, localization of maternal *nanos* (*nos*) mRNA to the germ plasm at the posterior pole of the early embryo is essential for patterning of the anterior-posterior body axis [1, 2]. In addition to producing sufficient Nos protein at the posterior to direct abdominal development, posterior localization of *nos* is required to activate its translation. When *nos* localization is abolished by mutations in germ plasm components like *oskar* (*osk*), *vasa* (*vas*), and *tudor* (*tud*), *nos* translation is repressed [3]. Consequently, the resulting embryos fail to develop abdominal segments. Posterior localization also facilitates the incorporation of *nos* RNA into the germline progenitor cells (pole cells) [4, 5], whose migration to the gonad requires *nos* function [6, 7].

While *nos* function requires localized *nos* RNA in the embryo, the process of *nos* localization occurs during oogenesis [2]. *nos* RNA is synthesized by the ovarian nurse cells that are connected to the oocyte anterior and accumulates in the early oocyte. Other developmentally important RNAs also accumulate in the early oocyte and several, including *bcd*, *osk*, and *gurken* (*grk*), become localized within the oocyte during midoogenesis [8]. By contrast, *nos* represents a class of RNAs including *cyclin B*, *germ cell-less* (*gcl*), and *polar granule component* (*pgc*), whose localization to the oocyte posterior does not occur until late in oogenesis, after the nurse cells have extruded or "dumped" their cytoplasmic contents into the oocyte [9–11]. Localization of these RNAs depends on the prior localization of *osk* RNA and the subsequent Osk protein-dependent assembly of the germ plasm at the oocyte posterior [10–12].

Genetic requirements for cytoplasmic dynein and/or kinesin in localization of *bcd*, *osk*, and *grk* mRNAs within *Drosophila* oocytes suggest that these RNAs are actively transported along microtubules [13–18]. This idea is consistent with evidence that microtubules are organized with their minus ends originating at the anterior and lateral oocyte cortex in midoogenesis, when *bcd*, *osk*, and *grk* achieve their distinct distributions [14, 19, 20]. Localization of these RNAs is abolished by drugs that depolymerize microtubules [18, 21–23]. Little is known, however, about the mechanism by which RNAs are localized at late stages of oogenesis. During this time, the bulk microtubule cytoskeleton shows no evidence of polarization. Rather, arrays of parallel microtubules assemble next to the cortex of the oocyte just prior to nurse cell dumping [19]. These subcortical microtubules are essential for ooplasmic streaming, the rapid movement of the oocyte cytoplasm that follows nurse cell dumping [24]. Ooplasmic streaming could provide a mechanism to transfer RNAs like *nos* from the nurse cell cytoplasm to the oocyte posterior, where they would be selectively trapped by association with the germ plasm. Consistent with this idea, ooplasmic streaming has been shown to facilitate posterior localization of *osk* transcripts injected into late oocytes [25]. However, physiologically relevant transport of endogenous mRNAs from the nurse cells to the posterior and posterior entrapment at late stages of oogenesis have yet to be investigated.

Once formed, *nos* RNA-germ plasm complexes must be maintained at the posterior. Actin-dependent anchoring of *osk* RNA at the posterior in midoogenesis has been inferred from the effects of *Tropomyosin II* and *moesin* mutations on *osk* localization and the partial release of *osk* RNA from the posterior upon actin depolymerization [14, 26–28]. In contrast, the role of the cytoskeleton in anchoring *nos* or other RNAs at the posterior cortex of late oocytes has not been elucidated.

A major impediment to the analysis of late-acting localization mechanisms is the inaccessibility of late stage

*Correspondence: lgavis@molbio.princeton.edu

oocytes to molecular probes. *Nos* RNA accumulates in the oocyte both during early and mid stages of oogenesis and later as the nurse cells contract, but posterior localization has not been observed until several hours after dumping is complete and only in rare examples ([2], E.R.G, unpublished data]. The fate of these two populations of *nos* RNA and the reason for the delayed appearance of *nos* at the posterior is not known. We have overcome the difficulty of detecting endogenous RNAs during late stages of oogenesis by adapting a method for fluorescent tagging of mRNA in vivo used to visualize *Ash1* RNA in yeast [29]. Previous analysis of localized RNAs in live *Drosophila* oocytes and embryos has relied on injection of fluorescently labeled synthetic RNAs [20, 25, 30, 31]. However, the behavior of these RNAs may be compromised by the labeling method and requirements for nuclear and/or nurse cell transport [20, 31]. We now report the first live visualization of endogenous RNA in *Drosophila* oocytes and embryos and the first in a multicellular system. As we show for *nos*, fluorescently labeled endogenous RNA is functionally indistinguishable from wild-type RNA.

We have used this new system to analyze the pathway of *nos* localization in late stage oocytes. Through pharmacological disruption, we have determined how microtubules and actin filaments, as well as the cytoplasmic movements they control, contribute to *nos* localization. We show that posterior localization of *nos* RNA initiates immediately upon nurse cell dumping and occurs by diffusion, entrapment, and actin-dependent anchoring of RNA entering the oocyte at this time. Unexpectedly, long range movement of *nos* RNA can occur in the absence of ooplasmic streaming. Our results demonstrate that diffusion/entrapment mechanisms can generate asymmetric RNA distributions in cell types that lack cytoskeletal polarity.

Results

GFP Labeling of *nos* RNA In Vivo

To investigate the *nos* localization pathway, we adapted a GFP-labeling system previously used for in vivo analysis of *Ash1* mRNA localization in yeast [29]. The strategy requires two components: a *nos* transgene carrying an insertion of six tandem copies of the stem-loop binding site for bacteriophage MS2 coat protein (MCP) in its 3′ UTR (*nos-(ms2)$_6$*) and a second transgene encoding an MCP-GFP fusion protein under control of the maternally active *hsp83* promoter. When the two transgenes are coexpressed, binding of MCP-GFP to its recognition motifs in *nos-(ms2)$_6$* RNA labels the RNA with GFP.

The *nos-(ms2)$_6$* transgene, either alone or combined with the *hsp83-MCP-GFP* transgene, completely rescues the *nos* mutant abdominal defect. GFP-labeled *nos-(ms2)$_6$* RNA (hereafter referred to as fluorescent *nos* RNA) is localized to the posterior pole of the early embryo and becomes incorporated into the pole cells (Figures 1A and 1D), as previously demonstrated for wild-type *nos* RNA by in situ hybridization. In addition, posterior localization of fluorescent *nos* RNA is disrupted in *osk* and *vas* mutants (data not shown), and the resulting embryos lack abdominal segments. By these criteria, fluorescent *nos* RNA behaves indistinguishably from wild-type *nos* RNA in its localization and translational regulation in the early embryo.

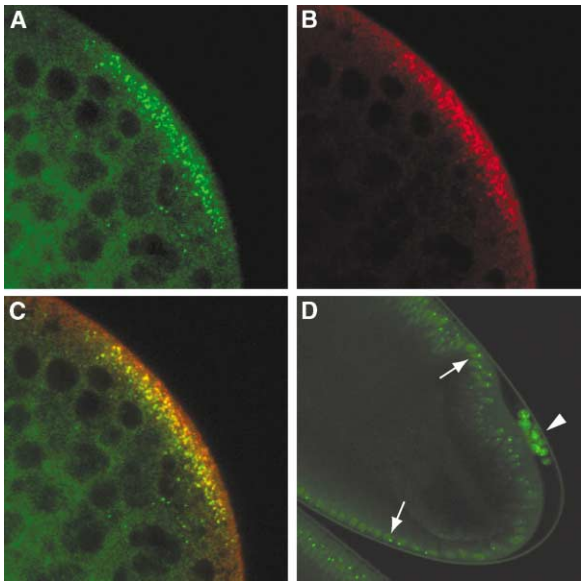

Figure 1. Fluorescent *nos* RNA Localization in Embryos

(A–C) Confocal images of fixed, preblastoderm embryo expressing MCP-GFP and *nos-(ms2)$_6$* RNA. Fluorescent *nos* RNA (green, [A]) colocalizes with Vas protein (red, [B]) as shown by the merged image (C). Similar results were obtained for wild-type *nos* RNA by using combined FISH and anti-Vas immunofluorescence (A. Vlasak and E.R.G., unpublished data).

(D) A live embryo with GFP-labeled (fluorescent) *nos* RNA in pole cells (arrowhead) during gastrulation. Since MCP-GFP bears a nuclear localization signal, MCP-GFP that is not bound to RNA enters the somatic nuclei (arrows).

From early to midoogenesis, the distribution of fluorescent *nos* in live egg chambers recapitulates the pattern previously observed for wild-type *nos* RNA by in situ hybridization [2, 32]. *Drosophila* oogenesis can be divided into 14 morphologically distinct stages in which the oocyte develops within an egg chamber surrounded by a somatic follicle cell epithelium [33]. Through stage 11, the oocyte remains connected at its anterior end to 15 interconnected nurse cells that synthesize *nos* and other maternal mRNAs. In early egg chambers, fluorescent *nos* RNA accumulates preferentially in the oocyte and is concentrated at the oocyte posterior (Figures 2A and 2D). During stages 8 and 9, the RNA accumulates in a ring at the anterior margin of the oocyte (Figures 2B and 2E). As for wild-type *nos*, this anterior accumulation is transient, and, by stage 10, there is no detectable localization of fluorescent *nos* RNA in the oocyte (Figures 2C and 2F). Taken together, these results demonstrate that fluorescent *nos* provides a valid proxy in the in vivo analysis of the *nos* mRNA localization pathway.

nos RNA Accumulates at the Oocyte Posterior during Nurse Cell Dumping

During the first half of oogenesis, mRNAs are steadily transferred from the nurse cells to the oocyte. Following stage 10, when the oocyte has enlarged to occupy half

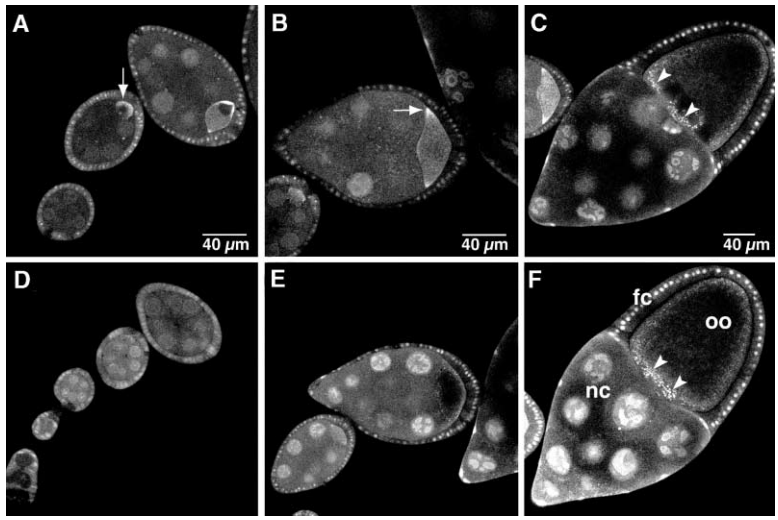

Figure 2. Fluorescent *nos* RNA Accumulates in Early Oocytes

(A–C) Confocal images of live egg chambers expressing both *nos-(ms2)$_6$* RNA and MCP-GFP.

(D–F) Control egg chambers expressing MCP-GFP alone. Due to the activity of the *hsp83* promoter, MCP-GFP is expressed in both the germline and follicle cells, whereas the *nos* promoter limits expression of *nos-(ms2)$_6$* RNA to the germline. MCP-GFP that is not bound to *nos-(ms2)$_6$* RNA enters both the nurse cell nuclei (nc) and the nuclei of follicle cells (fc) surrounding the oocyte (oo). Binding of MCP-GFP to *nos-(ms2)$_6$* RNA is epistatic to nuclear localization of MCP-GFP, as increasing the amount of *nos-(ms2)$_6$* RNA decreases the amount of MCP-GFP detected in nurse cell nuclei (data not shown). Fluorescent *nos* RNA is detected at the oocyte posterior in stage 4–6 egg chambers ([A], arrow), but not in comparably staged controls (D). (B and E) During stage 8, fluorescent *nos* RNA accumulates in a ring at the anterior margin of the oocyte (arrow). (C and F) By stage 10, fluorescent *nos* RNA is no longer localized within the oocyte. Arrowheads indicate autofluorescent yolk granules.

the volume of the egg chamber, an actin-dependent contraction of the nurse cells results in the rapid extrusion of nurse cell cytoplasm into the oocyte [34, 35]. Just prior to nurse cell dumping, the stage 10b oocyte initiates a vigorous microtubule-dependent streaming of its cytoplasm that continues until stage 13. Unlike the random, short-range cytoplasmic flows that occur in the oocyte during stages 8–10, ooplasmic streaming is coordinated such that the bulk ooplasm churns in a unidirectional flow [34, 36]. Both nurse cell dumping and ooplasmic streaming are faithfully reproduced in cultured egg chambers (see Movie 1 in the Supplemental Data available with this article online).

Substantial amounts of *nos* and other maternal mRNAs are presumed to enter the oocyte during stage 11 as a result of nurse cell dumping. While a minimal amount of fluorescent *nos* RNA is distinguishable at the posterior in ~50% of live stage 10b oocytes (see below), posterior localization is first detected reliably early in stage 11, immediately after the onset of dumping (Figures 3A and 3E). *nos* RNA continues to accumulate at the ooctye posterior as dumping proceeds (Figures 3B and 3F) and reaches a maximum level by stages 13–14 (Figures 3C and 3G). Posterior fluorescence is never detected in control egg chambers expressing MCP-GFP alone (Figure 3D), although autofluorescent yolk granules appear in MCP-GFP control oocytes and oocytes with both MCP-GFP and *nos-(ms2)$_6$* RNA (arrows in Figures 3E and 3F).

Posteriorly localized fluorescent *nos* RNA is particulate. A projection of confocal images taken successively through the depth of the oocyte reveals that fluorescent *nos* particles, ranging in size from 0.1 to 1 μm, are distributed in a cap around the posterior cortex (Figure 3H). The majority of these particles lie within superficial sections immediately below the follicle cell layer where the oocyte cortex resides, suggesting that they are associated with the cortex. Time-lapse confocal imaging of the oocyte posterior during stage 12 shows that *nos* particles are detected only at the posterior (Movie 2), suggesting that they form upon localization. These particles most likely form as *nos* RNA associates with the germ plasm since they are not detected in oocytes from *osk*, *vas*, *tud*, or *valois* mutants, in which posterior localization of wild-type *nos* is disrupted (data not shown). Furthermore, fluorescent *nos* RNA colocalizes with Vas protein in particles at the posterior pole of the early embryo (Figures 1A–1C).

Ooplasmic Streaming Promotes Efficient Localization of *nos* RNA

Our results show that *nos* RNA reaches the posterior of the oocyte much earlier than previously thought. The appearance of *nos* at the posterior concomitant with nurse cell dumping and ooplasmic streaming suggests that these cytoplasmic movements may provide the driving force behind *nos* localization. Nurse cell dumping and ooplasmic streaming are pharmacologically separable; dumping can be disrupted selectively by drugs that cause actin depolymerization [35], while ooplasmic streaming is blocked by drugs that depolymerize microtubules [24]. To determine whether localization of *nos* RNA can occur in the absence of ooplasmic streaming, egg chambers containing fluorescent *nos* RNA were dissected at stage 10b and cultured for 8 hr in the presence of the microtubule inhibitors colcemid or colchicine. Consistent with previous reports, stage 10b egg chambers treated with either of these inhibitors initiate nurse cell dumping and progress through oogenesis but show no evidence of ooplasmic streaming (Movie 3 and data not shown).

Surprisingly, fluorescent *nos* RNA can be detected at the posterior of the oocyte in 17/18 egg chambers cultured for 8 hr in the presence of colcemid (Figures 4B and 4D) and in 17/19 egg chambers treated with colchicine (data not shown). Time-lapse imaging of a representative colcemid-treated egg chamber shows that posterior accumulation of fluorescent *nos* RNA occurs after cessation of ooplasmic streaming (data not shown). By contrast, stage 10b egg chambers express-

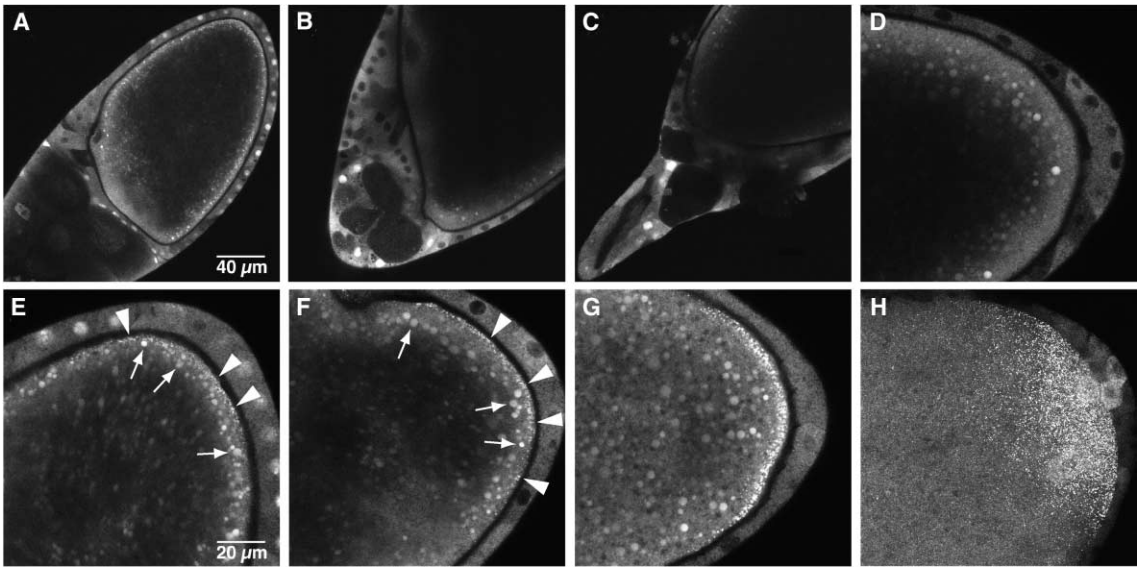

Figure 3. Fluorescent *nos* RNA Accumulation at the Oocyte Posterior Is Coincident with Nurse Cell Dumping

(A–C) Low-power confocal images of live egg chambers expressing both *nos-(ms2)*$_6$ RNA and MCP-GFP. The anterior view used for oocyte staging is shown: (A) stage 11, (B) stage 12, (C) stage 13.

(D) High-power image of the posterior of a live stage 13 egg chamber expressing MCP-GFP alone.

(E–G) High-power images of the live egg chambers in (A)–(C), respectively, showing the oocyte posterior. Arrowheads indicate fluorescent *nos* RNA accumulating at the posterior as oogenesis proceeds. Autofluorescent yolk particles are indicated by arrows.

(H) Z-series projection of the posterior end of a fixed stage 13 oocyte expressing fluorescent *nos* RNA. *Nos* RNA is apposed to the cortex, just below the follicle cell layer.

ing MCP-GFP alone never show posterior fluorescence after prolonged exposure to either colcemid or colchicine (data not shown).

To further confirm that the localization of fluorescent *nos* RNA observed in colcemid-treated egg chambers does not occur prior to inhibitor addition, we compared the amount of fluorescent RNA at the posterior of stage 10b oocytes immediately after dissection to the amount detected after the 8 hr inhibitor treatment. Nearly half (5/11) of the egg chambers examined directly after dissection completely lack posteriorly localized fluorescent *nos* RNA. The remainder show a minimal amount that is substantially less than that observed in egg chambers cultured for 8 hr with either microtubule inhibitor (data not shown). Therefore, accumulation of fluorescent *nos* RNA at the posterior must occur in the absence of ooplasmic streaming.

Consistent with the inhibition of ooplasmic streaming, cortical microtubules are no longer apparent after drug treatment is initiated (Figures 4E and 4F). Furthermore, *bcd* RNA localization is abolished under these conditions (data not shown). These results indicate that localization of fluorescent *nos* RNA in drug-treated oocytes is not due to residual microtubule activity. Moreover, microtubule-independent *nos* localization is inconsistent with directed transport, but it can be explained by a diffusion-based transport mechanism. Quantitation of posterior fluorescence intensity reveals that ~7% as much *nos* RNA is present at the oocyte posterior in drug-treated egg chambers as in mock-treated controls (compare Figures 4C and 4D). Thus, wild-type localization requires both microtubule-dependent and -independent events. Taken together, our data strongly support a role for ooplasmic streaming in enhancing diffusion-based transport to achieve wild-type posterior accumulation. We cannot, however, eliminate the possibility that directed transport is superimposed on diffusion for posterior localization. Finally, microtubules are not required for the stable association of *nos* RNA with the oocyte cortex, as fluorescent *nos* RNA remains at the posterior cortex in stage 12 egg chambers treated for 8 hr with colcemid (11/11) or colchicine (4/4; data not shown).

Nurse Cell Dumping Is Required for *nos* RNA Localization

Nurse cell dumping is readily inhibited by drugs that depolymerize microfilaments [35]. However, concomitant disruption of the cortical actin cytoskeleton within the oocyte could potentially affect stable anchoring of *nos* RNA at the posterior. We found that treatment of egg chambers with low concentrations of the actin depolymerizing agents latrunculin A (latA) or cytochalasin D (cytoD) abolishes dumping but does not affect oocyte cortical actin filaments or posterior localization of Vas-GFP (data not shown). We have therefore exploited this differential sensitivity to selectively examine the role of nurse cell dumping in *nos* RNA localization.

Egg chambers dissected at stage 10b were cultured for 8 hr in media containing either latA or cytoD at low concentration; both inhibitors gave similar results. A time-lapse movie of a representative latA-treated egg chamber shows that while nurse cell dumping fails to occur, ooplasmic streaming is unaffected (Movie 4). By contrast, mock-treated egg chambers progress normally through stage 13 of oogenesis. While fluorescent

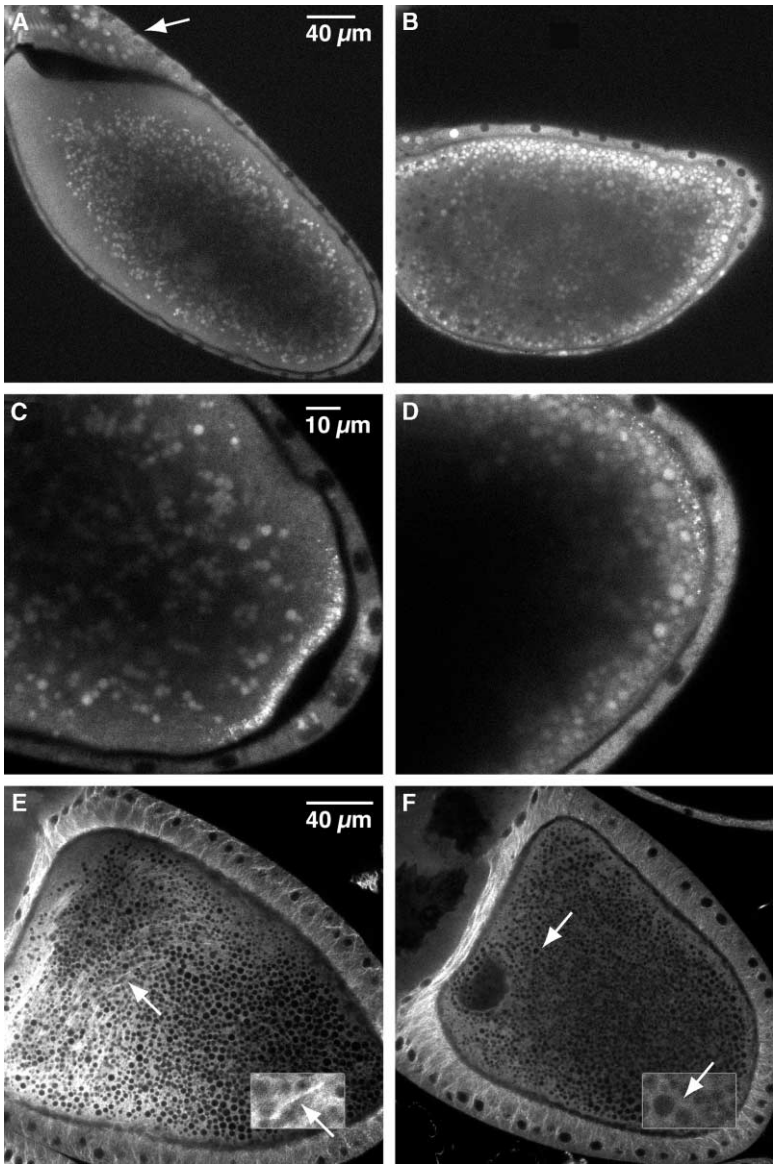

Figure 4. Microtubules Are Not Essential for, but Enhance Posterior Localization.

(A–F) Egg chambers were dissected at stage 10b, were cultured in either (A, C, and E) control media or in (B, D, and F) media containing 50 μg/ml colcemid and were imaged live. (A) A low-power image of an egg chamber after an 8 hr treatment in control media. The egg chamber develops through stage 13, undergoing both nurse cell dumping and ooplasmic streaming, as determined by the remnants of the nurse cells (arrow) and the uniform distribution of the ooplasm. (B) A low-power image of an egg chamber after treatment for 8 hr with colcemid. While this egg chamber underwent nurse cell dumping, ooplasmic streaming did not occur. In the absence of streaming, the ooplasm becomes stratified, with yolk granules near the cortex and the nurse cell cytoplasm more interior. (C) A high-power image of the posterior of the egg chamber shown in (A). Fluorescent *nos* RNA accumulates to wild-type levels at the posterior. (D) A high-power image of the posterior of the egg chamber shown in (B). Fluorescent *nos* RNA can still be detected at the posterior, although at reduced levels. In egg chambers cultured for 5 min, α-tubulin immunofluorescence shows that the cortical microtubule network ([E], arrow) is completely disrupted by colcemid ([F], arrow). The insets show enlargement of areas indicated by the arrows.

nos RNA accumulates normally at the posterior of the oocyte in mock-treated egg chambers, 10/24 latA-treated oocytes lack posteriorly localized RNA (Figures 5A and 5C). In the remaining egg chambers, a minimal amount of *nos* RNA can be detected at the posterior. This RNA was presumably localized prior to drug treatment since it appears comparable to that detected at the posterior in ~50% of stage 10b oocytes examined immediately after dissection. Furthermore, treatment of stage 12 egg chambers for 8 hr with latA at low concentration does not disrupt localization of fluorescent *nos* RNA that had already accumulated at the posterior ($n = 12/12$; Figures 5B and 5D). Thus, *nos* RNA can still form a stable association with the oocyte cortex under these conditions.

These results strongly suggest that the population of *nos* RNA localized to the oocyte posterior from stage 11 onward comes primarily from the stage 10b nurse cells and that *nos* RNA present in the oocyte prior to dumping makes little or no contribution to embryonic patterning. Furthermore, despite the fact that ooplasmic streaming continues, it is ineffective at promoting *nos* RNA localization in the absence of nurse cell dumping. While we cannot completely exclude actin-mediated transport of *nos* RNA, the long-range movement (>100 μm) observed for *nos* RNA is not consistent with actin-based transport [37]. Furthermore, the ability of ooplasmic streaming to enhance localization indicates that any contribution of actin filaments to *nos* transport must be minor.

Stable Anchoring of *nos* RNA Requires an Intact Actin Cytoskeleton

Previous analysis has shown that actin filaments play a role in maintaining *nos* RNA and germ plasm components at the posterior pole of the early embryo [38]. By contrast, depolymerization of actin filaments does not affect anchoring of injected *osk* RNA in late oocytes

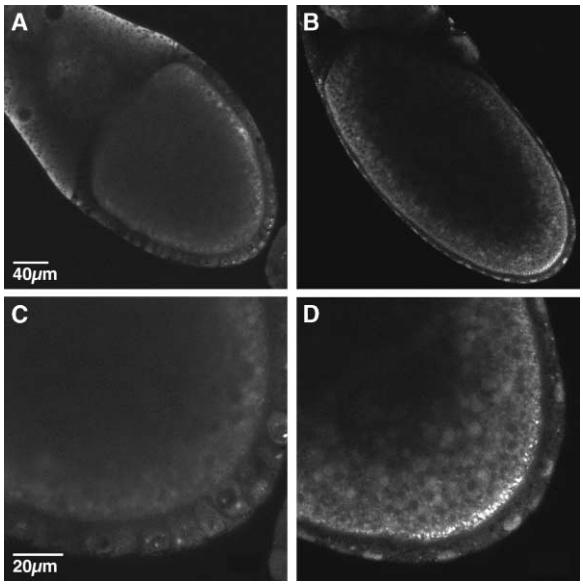

Figure 5. Nurse Cell Dumping Is Required for Posterior *nos* Localization

(A and B) Low-power confocal images of live egg chambers dissected at (A) stage 10b or (B) stage 12 and cultured for 8 hr in 420 ng/ml latrunculin A. Nurse cell dumping is blocked in both egg chambers, but the integrity of these egg chambers is unaffected.
(C) A high-power image of the posterior of the egg chamber shown in (A). No fluorescent RNA can be detected at the posterior.
(D) A high-power image of the posterior of the egg chamber shown in (B). RNA localized to the posterior prior to inhibitor treatment remains localized after the 8 hr treatment.

[25]. To determine if an association of *nos* RNA with the cortical actin cytoskeleton is established during oogenesis or only later at fertilization, we tested the effect of actin depolymerization on fluorescent *nos* RNA localization. Stage 12 egg chambers were cultured in cytoD at higher concentrations than those used to disrupt nurse cell dumping. As monitored with GFP-actin, fragmentation of actin filaments and detatchment from the cortex begins shortly after the addition of cytoD (Movie 5). Similarly, in egg chambers expressing fluorescent *nos* RNA, the RNA detaches from the posterior cortex after the addition of cytoD (n = 13) but is unaffected in mock-treated samples. Interestingly, the RNA is released as a large aggregate that is immediately swept away by the streaming ooplasm (Figures 6A–6F; Movie 6). This aggregate contains fluorescent *nos* RNA and is not labeled in cytoD-treated egg chambers expressing MCP-GFP alone (data not shown).

To determine whether *nos* RNA detatches independently of the germ plasm, we examined the effect of cytoD on posterior localization of the germ plasm in egg chambers expressing Vas-GFP. Like fluorescent *nos* RNA, Vas-GFP also detaches from the posterior cortex as a large aggregate (Movie 7). Fluorescent *nos* RNA and Vas-GFP begin to detach from the posterior cortex at approximately the same time after treatment with cytoD (29 ± 12 min for *nos* [n = 13]; 32 ± 5 min for Vas-GFP [n = 11]). This coincident release suggests that fluorescent *nos* RNA and Vas-GFP protein detach from the posterior cortex as part of the same aggregate. Taken together, the above results indicate that *nos* RNA is anchored to the actin cytoskeleton during oogenesis through its association with the germ plasm.

Discussion

A variety of mechanisms, including directed transport along microtubules or microfilaments, diffusion with localized entrapment, and generalized RNA degradation coupled to localized protection, have been proposed for intracellular localization of mRNAs. Using a two component system that generates GFP-labeled RNA in vivo, we show that a microtubule-independent mechanism based on diffusion and entrapment mediates posterior localization of *nos* RNA during late stages of *Drosophila* oogenesis. Our results reveal that *nos* RNA deposited at the anterior of the oocyte during nurse cell dumping can accumulate at the posterior in the absence of functional microtubules and the ooplasmic movements they control. Notably, because the level of *nos* RNA at the posterior cortex increases continuously after the onset of nurse cell dumping, protection from RNA degradation cannot account for *nos* localization, in contrast to a previously proposed model [39]. Entrapment of *nos* at the posterior occurs by its association with the localized germ plasm and is enhanced by microtubule-dependent ooplasmic streaming. The entire *nos* RNA-germ plasm complex is anchored to the cortex of the oocyte by the actin cytoskeleton, which maintains posterior localization in the face of ooplasmic streaming.

We propose that the germ plasm-dependent, late posterior localization of *cyclin B*, *gcl*, and *pgc* RNAs occurs by this same mechanism [9–11]. Synthetic *osk* RNA can localize to the posterior after injection into stage 10/11 oocytes [25], although it is not known whether endogenous *osk* RNA uses the late acting pathway or how *osk* is trapped and anchored at this time. Because the microtubule-dependent localization of *osk* during stages 8 and 9 of oogenesis is essential for germ plasm assembly prior to nurse cell dumping [13, 22, 23] and the subsequent localization of *nos* RNA after nurse cell dumping, the significance of late *osk* localization is not clear. It is possible that additional posterior accumulation of *osk* at later stages may amplify the germ plasm in the expanding oocyte.

Diffusion-based mechanisms may also play an important role in localization of maternal RNAs in amphibian and fish eggs. RNAs like Xcat2, which encodes a Nos-related protein, as well as Xlsirts and Xwnt11 are initially present throughout the *Xenopus* oocyte but become localized to the germ plasm within the mitochondrial cloud early in oogenesis without any decrease in their overall abundance [40, 41]. This localization does not require microtubules or microfilaments [42]. Similarly, the microtubule- and actin-independent translocation of *zorba* and *Vg1* RNAs to the animal pole of the zebrafish oocyte is consistent with diffusion-based localization [43]. In addition, cytoplasmic streaming has been implicated in localization of RNAs to the zebrafish blastoderm [44].

Posterior localization of *nos* is inefficient, as only 4% of the total *nos* RNA pool is found at the posterior of the embryo [32]. Since the amount of localized *nos* can

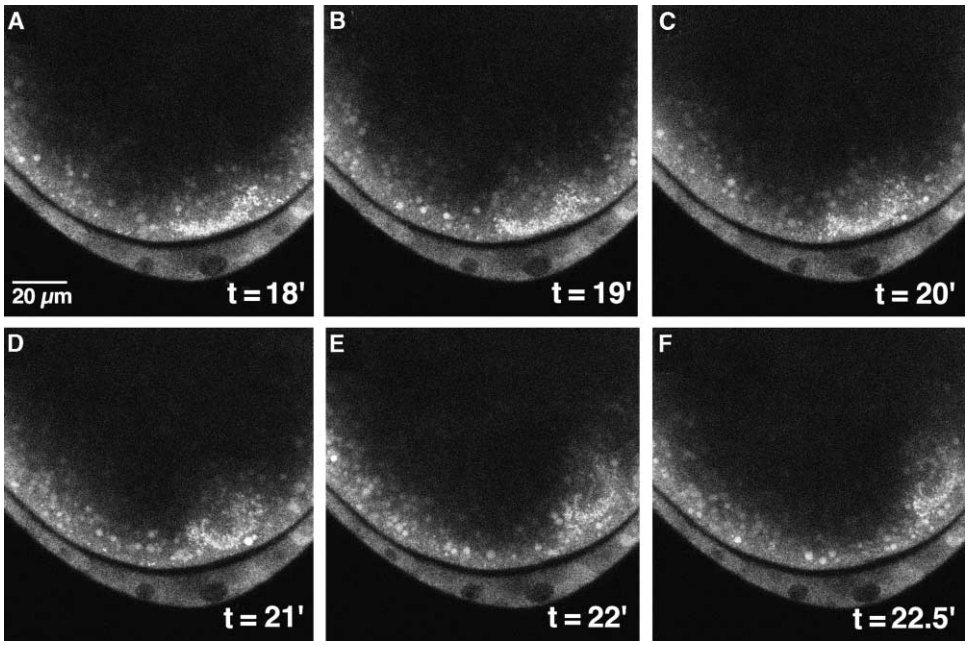

Figure 6. Stable Anchoring of Fluorescent *nos* RNA Requires an Intact Cortical Actin Cytoskeleton

(A–F) Time-lapse confocal images of a stage 12 egg chamber cultured in the presence of 10 μg/ml cytochalasin D. The elapsed time after the addition of inhibitor is indicated. (A–D) Fluorescent *nos* RNA is still associated with the posterior cortex 21 min after inhibitor treatment is initiated. By 22 min, (E) fluorescent *nos* fully detaches, and by 22.5 min, (F) fluorescent *nos* is swept away as an aggregate (also see Movie 6). Vas-GFP protein detaches from the posterior cortex in cytochalasin D-treated egg chambers in a similar manner (see Movie 7).

be augmented by increasing the *nos* gene dosage [1], germ plasm is not limiting. Furthermore, the ability of ooplasmic streaming to increase posterior accumulation indicates that access of *nos* RNPs to the germ plasm rather than their affinity for germ plasm binding determines the efficiency of entrapment. Entrapment of a critical mass of *nos* RNA must be achieved, however, since the number of abdominal segments formed by the embryo depends on the amount of *nos* RNA localized at the posterior [32, 45]. The failure to accumulate *nos* RNA at the posterior when nurse cell dumping is inhibited argues that *nos* RNA entering the oocyte in early to midoogenesis is not sufficient for wild-type *nos* function. Rather, nurse cell dumping plays a key role in providing the concentration of *nos* RNA required to promote sufficient RNA-germ plasm complex formation for abdominal patterning. Based on the behavior of *nos* RNA derivatives whose localization is partially compromised [45], we estimate that the amount of *nos* RNA localized by diffusion alone (as in colcemid-treated egg chambers, Figure 4D) would generate several abdominal segments at most. Thus, by enhancing posterior entrapment, ooplasmic streaming is predicted to make a critical contribution to abdominal patterning.

Inefficient localization of *nos* has potentially dire consequences, since production of Nos throughout the embryo causes lethal patterning defects. Unlocalized *nos* RNA is tolerated, however, by the tight coupling of *nos* translation to its localization [3]. In contrast to *nos*, RNAs like *cyclin B* may be ideally served by an inefficient localization mechanism. While entrapment at the posterior promotes incorporation of *cyclin B* into the pole cells for its later use in germ cell mitosis, synthesis of cyclin B protein throughout the embryo is essential for early embryogenesis [12, 46].

The diffusion and entrapment mechanism responsible for late posterior localization of *nos* and other RNAs contrasts with RNA localization mechanisms that act earlier in oogenesis. Microtubule- and dynein-dependent localization of *bcd* is efficient, so that nearly all of the *bcd* RNA within the embryo resides at the anterior pole [32]. Comparison of our results with results from previous studies of *bcd* localization reveals differences in the formation of particles by these two RNAs that may contribute to differences in the efficiency of their localization. Following injection into nurse cells, in vitro-synthesized fluorescent *bcd* RNA forms particles that are transported into the oocyte and are localized to the anterior cortex. The large size of the particles (0.5–1 μm diameter) suggests that they contain many *bcd* molecules [20]. Colocalization of these particles with Exuperentia protein, whose role in *bcd* localization has been defined genetically, and the microtubule dependence of their movement suggests that they are bona fide transport RNPs [20]. The ability of *bcd* to form large RNPs could contribute significantly to its efficient localization since coupling of a single RNP to a microtubule would permit simultaneous transport of many *bcd* molecules. While we have detected similar particles in the nurse cells of egg chambers expressing in vivo GFP-labeled *bcd* RNA (K.M.F. and E.R.G., unpublished), we do not detect particles of fluorescent *nos* RNA either in nurse cells or within the bulk ooplasm at any stage of oogenesis. Genetic and biochemical analysis suggest that *nos* RNA is indeed translocated to the posterior as an RNP ([5, 32, 47], B. Yao and E.R.G., unpublished data). The

lack of visible *nos* transport particles can be explained if individual *nos* RNA-protein complexes are the preferred substrate for germ plasm association. Whereas *bcd* RNPs appear to be organized into higher-order complexes prior to localization, a similar organization of multiple *nos* RNPs into larger complexes may occur only upon association with the germ plasm.

Once *nos* RNA is incorporated into the germ plasm, maintenance at the posterior requires linkage to the cortical actin cytoskeleton. When released from the cortex by actin depolymerization, *nos* RNA, together with the germ plasm, remains coalesced in a large aggregate that is swept away intact from the posterior by ooplasmic streaming movements. This behavior suggests that the germ plasm, including its associated mRNAs, maintains a structural integrity independent of the actin cytoskeleton. Structural integrity may be mediated by the Short Osk isoform since smaller aggregates containing Short Osk, Vas, and *osk* mRNA appear when Short Osk is released from the posterior cortex by mutations in the Long Osk isoform [48]. Microfilaments contribute to the continued localization of germ plasm after fertilization, as actin depolymerization results in partial loss of *nos* RNA as well as Osk and Vas proteins from the posterior pole of the embryo [38]. As embryogenesis proceeds, aggregation of the germ plasm may ensure its segregation to the pole cells when the actin cytoskeleton reorganizes for pole cell formation [49].

Experimental Procedures

Fly Stocks

The following mutants and allelic combinations were used: *y* w^{67c23} [50], nos^{BN} [2], osk^{54}/osk^{150} [51], vas^{PD}/vas^{D1} [51, 52], tud^{WC8} [52], vls^{PE}/vls^{PG} [52, 53]. Transgenic strains generated by others include *Vas-GFP* (gift of C. Yohn and R. Lehmann), *UASp2-GFP-actin* [54], and *mat67.15* (GAL4-VP16 under the control of the maternal α-tubulin promoter [55]). Ovarian expresion of GFP-actin was achieved in females carrying both the *UASp2-GFP-actin* and *mat67.15* transgenes.

Construction of Transgenes and Generation of Transgenic Lines

hsp83-MCP-GFP

The P element plasmid pCaS-P_{hsp83}-MCP-GFP was generated by insertion of sequences encoding an NLS followed by a C-terminal fusion of EGFP to MCP [29] downstream of the *hsp83* promoter in the CaSpeR-hs83 plasmid [56]. 3′ UTR and 3′ genomic sequences were provided by the α-tubulin gene [57]. Details are provided in the Supplemental Data available with this article online.

nos-(ms2)$_6$

The P element plasmid pCaS2-nos-$(ms2)_6$ contains a 4.3 kb fragment of genomic *nos* sequence, including the *nos* promoter. Six tandemly repeated ms2 stem-loop binding sites derived from pSL-MS2-6 [29] were inserted into the *nos* 3′ UTR, 500 bases downstream of the *nos* stop codon. Details are provided in the Supplemental Data.

Live Imaging and Inhibitor Treatment

All images were captured with a Zeiss LSM 510 confocal microscope. Egg chambers were staged according to Spradling [33]. To examine the distribution of *nos* RNA throughout oogenesis and for all time-lapse movies, ovaries from well-fed females were dissected in Schneider's insect culture medium (GIBCO-BRL). Individual egg chambers were dissected away from ovarioles by using fine tungsten needles, then rinsed once in Schneider's medium. An individual egg chamber was then mounted on an uncoated #1.5 glass bottom culture dish (MatTek) in 200 μl Schneider's medium. Slight back pressure was applied by laying a 4 mm^2 square #1 glass coverslip (Corning) on top of the egg chamber with Dumont #5 Tweezers (EMS). Due to rapid decay of early egg chambers, imaging prior to stage 10A was limited to 10 min. From stage 10B onward, egg chambers were viable under these conditions for more than 8 hr. Live embryos were imaged in 27S halocarbon oil, and double stick tape was used to maintain spacing.

For inhibitor treatment, stock solutions of colcemid, colchicine, cytochalasin D, and latrunculin A (Sigma) were prepared in 100% ETOH. Colcemid and colchicine were used at a final concentration of 50 μg/ml and 20 μg/ml, respectively. To inhibit nurse cell dumping, latrunculin A and cytochalasin D were used at a final concentration of 420 ng/ml (1 μM) and 1 μg/ml, respectively; to disrupt cortical actin, cytochalasin D was added to a final concentration of 10 μg/ml. Preparation of egg chambers for time-lapse imaging was carried out as described above, with the addition of inhibitor or vehicle to the medium after mounting. For all other experiments, appropriate stage egg chambers were individually dissected in Schneider's medium, rinsed once, and added to 1 ml Schneider's medium containing either the inhibitor or an equal volume of ETOH. Egg chambers were then incubated at room temperature in the dark with rotation for at least 8 hr, then imaged on a glass slide without back pressure in order to maintain egg chamber integrity.

Immunofluorescence

Ovaries from well-fed females were dissected in Schneider's medium containing either 50 μg/ml colcemid, 20 μg/ml colchicine, or an equal volume of ETOH. Egg chambers were rinsed once in the respective medium, incubated with rotation for 5 min in the dark at room temperature, then fixed for 15 min in 4% paraformaldehyde/PBS. Fixed ovaries were rinsed four times in PBS, incubated for 2 hr at room temperature in BBT (PBS/0.1% BSA/0.1% Triton X-100), then incubated overnight at 4°C in 1:100 FITC-conjugated mouse α-tubulin Ab (Sigma). Ovaries were washed twice for 10 min with BBT, once with PBST (PBS/0.1% Tween 20), mounted in PBST, and imaged.

Embryos containing fluorescent *nos* RNA were fixed for 20 min in 4% paraformaldehyde/PBS, devitellinized with rapid shaking in 1:4 heptane:MeOH, and washed with MeOH. Following rehydration into BBT, immunostaining was carried out as above. Embryos were incubated with 1:1000 rabbit anti-Vas [58] overnight at 4°C and 1:1000 Alexa Fluor 568 goat anti-rabbit (Molecular Probes) for 2 hr at room temperature.

Supplemental Data

Supplemental Data including the movies (Movies 1–7) referred to in the text and detailed descriptions of the methods used in transgene construction and fluorescence quantitation are available at http://www.current-biology.com/content/supplemental.

Acknowledgments

We thank Rob Singer for his generosity with reagents and advice on GFP labeling of RNA, Chris Yohn, Ruth Lehmann, Lynn Cooley, and Eric Wieschaus for providing fly stocks, Joe Goodhouse and Eric Wieschaus for assistance with confocal microscopy, and Tim Weil for assistance with quantitation. We are also grateful to Ira Clark and Eric Wieschaus for helpful discussions and comments on the manuscript. This work was funded by American Cancer Society grant #RPG-97-022.

Received: April 10, 2003
Revised: May 12, 2003
Accepted: May 14, 2003
Published: July 15, 2003

References

1. Gavis, E.R., and Lehmann, R. (1992). Localization of *nano*s RNA controls embryonic polarity. Cell *71*, 301–313.
2. Wang, C., Dickinson, L.K., and Lehmann, R. (1994). Genetics of *nanos* localization in *Drosophila*. Dev. Dyn. *199*, 103–115.
3. Gavis, E.R., and Lehmann, R. (1994). Translational regulation of *nanos* by RNA localization. Nature *369*, 315–318.

4. Wang, C., and Lehmann, R. (1991). *Nanos* is the localized posterior determinant in *Drosophila*. Cell *66*, 637–647.
5. Gavis, E.R., Curtis, D., and Lehmann, R. (1996). Identification of cis-acting sequences that control *nanos* RNA localization. Dev. Biol. *176*, 36–50.
6. Kobayashi, S., Yamada, M., Asaoka, M., and Kitamura, T. (1996). Essential role of the posterior morphogen *nanos* for germline development in *Drosophila*. Nature *380*, 708–711.
7. Forbes, A., and Lehmann, R. (1998). Nanos and Pumilio have critical roles in the development and function of *Drosophila* germline stem cells. Development *125*, 679–690.
8. Bashirullah, A., Cooperstock, R.L., and Lipshitz, H.D. (1998). RNA localization in development. Annu. Rev. Biochem. *67*, 335–394.
9. Dalby, B., and Glover, D.M. (1992). 3′ non-translated sequences in *Drosophila* cyclin B transcripts direct posterior pole accumulation late in oogenesis and peri-nuclear association in syncytial embryos. Development *115*, 989–997.
10. Jongens, T.A., Hay, B., Jan, L.Y., and Jan, Y.N. (1992). The *germ cell-less* gene product: a posteriorly localized component necessary for germ cell development in *Drosophila*. Cell *70*, 569–584.
11. Nakamura, A., Amikura, R., Mukai, M., Kobayashi, S., and Lasko, P. (1996). Requirement for a noncoding RNA in *Drosophila* polar granules for germ cell establishment. Science *274*, 2075–2079.
12. Raff, J.W., Whitfield, W.G.F., and Glover, D.M. (1990). Two distinct mechanisms localise cyclin B transcripts in syncytial *Drosophila* embryos. Development *110*, 1249–1261.
13. Brendza, R.P., Serbus, L.R., Duffy, J.B., and Saxton, W.M. (2000). A function for kinesin I in the posterior transport of *oskar* mRNA and Staufen protein. Science *289*, 2120–2122.
14. Cha, B.-J., Serbus, L.R., Koppetsch, B.S., and Theurkauf, W.E. (2002). Kinesin I-dependent cortical exclusion restricts pole plasm to the oocyte posterior. Nat. Cell Biol. *4*, 592–598.
15. Palacios, I.M., and St Johnston, D. (2002). *Kinesin light chain*-independent function of the *Kinesin heavy chain* in cytoplasmic streaming and posterior localisation in the *Drosophila* oocyte. Development *129*, 5473–5485.
16. Januschke, J., Gervais, L., Dass, S., Kaltschmidt, J.A., Lopez-Schier, H., St Johnston, D., Brand, A.H., Roth, S., and Guichet, A. (2002). Polar transport in the *Drosophila* oocyte requires Dynein and Kinesin I cooperation. Curr. Biol. *12*, 1971–1981.
17. Duncan, J.E., and Warrior, R. (2002). The cytoplasmic Dynein and Kinesin motors have interdependent roles in patterning the *Drosophila* oocyte. Curr. Biol. *12*, 1982–1991.
18. MacDougall, N., Clark, A., MacDougall, E., and Davis, I. (2003). *Drosophila gurken* (TGFalpha) mRNA localizes as particles that move within the oocyte in two dynein-dependent steps. Dev. Cell *4*, 307–319.
19. Theurkauf, W.E., Smiley, S., Wong, M.L., and Alberts, B.M. (1992). Reorganization of the cytoskeleton during *Drosophila* oogenesis: implications for axis specification and intercellular transport. Development *115*, 923–936.
20. Cha, B.J., Koppetsch, B.S., and Theurkauf, W.E. (2001). In vivo analysis of *Drosophila bicoid* mRNA localization reveals a novel microtubule-dependent axis specification pathway. Cell *106*, 35–46.
21. Pokrywka, N.J., and Stephenson, E.C. (1991). Microtubules mediate the localization of *bicoid* RNA during *Drosophila* oogenesis. Development *113*, 55–66.
22. Pokrywka, N.J., and Stephenson, E.C. (1995). Microtubules are a general component of mRNA localization systems in *Drosophila* oocytes. Dev. Biol. *167*, 363–370.
23. Clark, I., Giniger, E., Ruohola-Baker, H., Jan, L.Y., and Jan, Y.N. (1994). Transient posterior localization of a kinesin fusion protein reflects anteroposterior polarity of the *Drosophila* oocyte. Curr. Biol. *4*, 289–300.
24. Gutzeit, H.O. (1986). The role of microtubules in the differentiation of ovarian follicles during vitellogenesis in *Drosophila*. W. Roux's Arch. Dev. Biol. *195*, 173–181.
25. Glotzer, J.B., Saffrich, R., Glotzer, M., and Ephrussi, A. (1997). Cytoplasmic flows localize injected *oskar* RNA in *Drosophila* oocytes. Curr. Biol. *7*, 326–337.
26. Erdélyi, M., Michon, A.-M., Guichet, A., Glotzer, J.B., and Ephrussi, A. (1995). Requirement for *Drosophila* cytoplasmic tropomyosin in *oskar* mRNA localization. Nature *377*, 524–527.
27. Polesello, C., Delon, I., Valenti, P., Ferrer, P., and Payre, F. (2002). Dmoesin controls actin-based cell shape and polarity during *Drosophila melanogaster* oogenesis. Nat. Cell Biol. *4*, 782–789.
28. Jankovics, F., Sinka, R., Lukacsovich, T., and Erdelyi, M. (2002). MOESIN crosslinks actin and cell membrane in *Drosophila* oocytes and is required for OSKAR anchoring. Curr. Biol. *12*, 2060–2065.
29. Bertrand, E., Chartrand, P., Schaefer, M., Shenoy, S.M., Singer, R.H., and Long, R.M. (1998). Localization of ASH1 mRNA particles in living yeast. Mol. Cell *2*, 437–445.
30. Wilkie, G.S., and Davis, I. (2001). *Drosophila wingless* and pair-rule transcripts localize apically by dynein-mediated transport of RNA particles. Cell *105*, 209–219.
31. Bullock, S.L., and Ish-Horowicz, D. (2001). Conserved signals and machinery for RNA transport in *Drosophila* oogenesis and embryogenesis. Nature *414*, 611–616.
32. Bergsten, S.E., and Gavis, E.R. (1999). Role for mRNA localization in translational activation but not spatial restriction of *nanos* RNA. Development *126*, 659–669.
33. Spradling, A.C. (1993). Developmental genetics of oogenesis. In The Development of *Drosophila melanogaster*, Volume I, M. Bate and A. Martinez Arias, eds. (Cold Spring Harbor: Cold Spring Harbor Press), pp. 1–70.
34. Gutzeit, H.O., and Koppa, R. (1982). Time-lapse film analysis of cytoplasmic streaming during late oogenesis of *Drosophila*. J. Embryol. Exp. Morphol. *67*, 101–111.
35. Gutzeit, H.O. (1986). The role of microfilaments in cytoplasmic streaming in *Drosophila* follicles. J. Cell Sci. *80*, 159–169.
36. Theurkauf, W.E. (1994). Premature microtubule-dependent cytoplasmic streaming in *cappuccino* and *spire* mutant oocytes. Science *265*, 2093–2096.
37. Langford, G. (1995). Actin- and microtubule-dependent organelle motors: interrelationships between the two motility systems. Curr. Opin. Cell Biol. *7*, 82–88.
38. Lantz, V.A., Clemens, S.E., and Miller, K.G. (1999). The actin cytoskeleton is required for maintenance of posterior pole plasm components in the *Drosophila* embryo. Mech. Dev. *85*, 111–122.
39. Dahanukar, A., and Wharton, R.P. (1996). The Nanos gradient in *Drosophila* embryos is generated by translational regulation. Genes Dev. *10*, 2610–2620.
40. Kloc, M., Larabell, C., Chan, A.P., and Etkin, L.D. (1998). Contribution of METRO pathway localized molecules to the organization of the germ cell lineage. Mech. Dev. *75*, 81–93.
41. MacArthur, H., Bubunenko, M., Houston, D.W., and King, M.L. (1999). Xcat2 RNA is a translationally sequestered germ plasm component in *Xenopus*. Mech. Dev. *84*, 75–88.
42. Kloc, M., Larabell, C., and Etkin, L.D. (1996). Elaboration of the messenger transport organizer pathway for localization of RNA to the vegetal cortex of *Xenopus* oocytes. Dev. Biol. *180*, 119–130.
43. Bally-Cuif, L., Schatz, W.J., and Ho, R.K. (1998). Characterization of the zebrafish Orb/CPEB-related RNA binding protein and localization of maternal components in the zebrafish oocyte. Mech. Dev. *77*, 31–47.
44. Maegawa, S., Yasuda, K., and Inoue, K. (1999). Maternal mRNA localization of zebrafish DAZ-like gene. Mech. Dev. *81*, 223–226.
45. Gavis, E.R., Lunsford, L., Bergsten, S.E., and Lehmann, R. (1996). A conserved 90 nucleotide element mediates translational repression of *nanos* RNA. Development *122*, 2791–2800.
46. Dalby, B., and Glover, D.M. (1993). Discrete sequence elements control posterior pole accumulation and translational repression of maternal cyclin B RNA in *Drosophila*. EMBO J. *12*, 1219–1227.
47. Bergsten, S.E., Huang, T., Chatterjee, S., and Gavis, E.R. (2001). Recognition and long-range interactions of a minimal *nanos* RNA localization signal element. Development *128*, 427–435.
48. Vanzo, N.F., and Ephrussi, A. (2002). Oskar anchoring restricts pole plasm formation to the posterior of the *Drosophila* oocyte. Development *129*, 3705–3714.
49. Warn, R.M., Smith, L., and Warn, A. (1985). Three distinct distributions of F-actin occur during the divisions of polar surface

caps to produce pole cells in *Drosophila* embryos. J. Cell Biol. *100*, 1010–1015.
50. Lindsley, D.L., and Zimm, G.G. (1992). The genome of *Drosophila melanogaster* (San Diego: Academic Press, Inc.).
51. Lehmann, R., and Nüsslein-Volhard, C. (1991). The maternal gene *nanos* has a central role in posterior pattern formation of the *Drosophila* embryo. Development *112*, 679–691.
52. Schüpbach, T., and Wieschaus, E. (1986). Maternal-effect mutations altering the anterior-posterior pattern of the *Drosophila* embryo. W. Roux's Arch. Dev. Biol. *195*, 302–317.
53. Schüpbach, T., and Wieschaus, E. (1989). Female sterile mutations on the second chromosome of *Drosophila melanogaster*. I. Maternal effect mutations. Genetics *121*, 101–117.
54. Kelso, R.J., Hudson, A.M., and Cooley, L. (2002). *Drosophila* Kelch regulates actin organization via Src64-dependent tyrosine phosphorylation. J. Cell Biol. *156*, 703–713.
55. Hunter, C., and Wieschaus, E. (2000). Regulated expression of nullo is required for the formation of distinct apical and basal adherens junctions in the *Drosophila* blastoderm. J. Cell Biol. *150*, 391–401.
56. Govind, S., Brennan, L., and Steward, R. (1993). Homeostatic balance between dorsal and cactus proteins in the *Drosophila* embryos. Development *117*, 135–148.
57. Theurkauf, W.E., Baum, H., Bo, J., and Wensink, P.C. (1986). Tissue-specific and constitutive alpha-tubulin genes of *Drosophila melanogaster* code for structurally distinct proteins. Proc. Natl. Acad. Sci. USA *83*, 8477–8481.
58. Hay, B., Jan, L.H., and Jan, Y.N. (1990). Localization of *vasa*, a component of *Drosophila* polar granules, in maternal-effect mutants that alter embryonic anteroposterior polarity. Development *109*, 425–433.